Animal Nutrition 17 (2024) 397–407

Contents lists available at ScienceDirect

Animal Nutrition

journal homepage: http://www.keaipublishing.com/en/journals/aninu/

Original Research Article

Excessive level of dietary insect protein negatively changed growth metabolomic and transcriptomic profiles of largemouth bass (*Micropterus salmoides*)

Hao Sun [a, b], Wenjing Dong [a, b], Guanglun He [a, b], Yong Long [c], Yuanfa He [a, b], Yongjun Chen [a, b], Shimei Lin [a, b, *]

[a] College of Fisheries, Southwest University, Chongqing 400715, China
[b] College of Fisheries, Key Laboratory of Freshwater Fish Reproduction and Development (Ministry of Education), Southwest University, Chongqing 400715, China
[c] State Key Laboratory of Freshwater Ecology and Biotechnology, Institute of Hydrobiology, Chinese Academy of Sciences, Wuhan 430072, China

ARTICLE INFO

Article history:
Received 29 October 2023
Received in revised form
23 December 2023
Accepted 18 March 2024
Available online 19 April 2024

Keywords:
Hermetia illucens
Growth
Transcriptome
Metabolomic effect
Micropterus salmoides

ABSTRACT

Hermetia illucens (HI) meal is a promising substitute for fish meal (FM) in the feeds of farmed fish. However, the impacts of dietary HI meal on largemouth bass (LMB) remain unknown. In this study, we formulated three isonitrogenous and isolipid diets with 0% (HI0, control), 20% (HI20) and 40% (HI40) of FM substituted by HI meal. A total of 270 juvenile largemouth bass with an initial body weight of 10.02 ± 0.03 g were used (30 fish per tank). After an 80-day feeding trial, the fish fed with the HI40 diet demonstrated decreased growth performance and protein efficiency ratio (PER), and increased liver oxidative indices and lipid accumulation compared to the control ($P < 0.05$). Transcriptomic analysis revealed the effects of high dietary HI meal on liver gene expression. Consistent with the reduced growth and disturbed liver oxidative status, the upregulated genes were enriched in the biological processes associated with protein catabolism and endoplasmic reticulum (ER) stress; while the downregulated genes were enriched in cellular proliferation, growth, metabolism, immunity and maintenance of tissue homeostasis. Differential metabolites in the liver samples were also identified by untargeted metabolomic assay. The results of joint transcriptomic–metabolomic analyses revealed that the pathways such as one carbon pool by folate, propanoate metabolism and alpha-linolenic acid metabolism were disturbed by high dietary HI meal. In summary, our data revealed the candidate genes, metabolites and biological pathways that account for the adverse effects of high HI meal diet on the growth and health of LMB.

1. Introduction

As global fish production continues to grow, the need to find more sustainable feed sources to provide for the nutritional needs of fish is critical. In terms of protein, existing diets are being replaced by healthier and more sustainable non-conventional sources of protein. Currently, insects have emerged as promising protein sources with nutritional and functional advantages, and already were used in the feed industry (Marco et al., 2015; Mohan et al., 2022; Yu et al., 2020). Black soldier fly (*Hermetia illucens* [HI]) especially has gained special attention in aquaculture owing to its high protein content and high feed conversion efficiency (Cardinaletti et al., 2019). More importantly, the inclusion of

* Corresponding author.
E-mail address: linsm@swu.edu.cn (S. Lin).
Peer review under responsibility of Chinese Association of Animal Science and Veterinary Medicine.

Production and Hosting by Elsevier on behalf of KeAi

https://doi.org/10.1016/j.aninu.2024.03.014

H. illucens in aquafeeds has been successfully achieved, and varies substantially depending upon fish species, diet composition, *H. illucens* processing and the source of food materials ingested by the larvae (Mohan et al., 2022). Prior research has indicated that the utilization of insect-derived protein sources may have an impact not only on the growth of fish, but also on their digestive capabilities and immune response (Chu et al., 2020; Fischer et al., 2022). However, limited information is available about response to partial diet replacement with *H. illucens* in non-insectivorous species.

In addition to growth-related metrics, the evaluation of insect meal in fish feed should consider any potential effects on metabolic, health, and safety issues (Antonopoulou et al., 2019). The liver, as the metabolic hub in the body, assumes the responsibility of regulating and coordinating a multitude of physiological processes. Additionally, it serves as a crucial "metabolic clearing house", playing a pivotal role in maintaining bodily homeostasis and facilitating detoxification. Liver diseases have emerged as a malady that affects animal productivity, and are often caused by unreasonable nutrition and feed as well as water quality. Fish species differences in hepatocellular function, toxicity and adaptation to protein sources are underappreciated, particularly in the absence of clinical trial data. Recently, the source of dietary protein has been suggested to play an important role in modulating health biomarkers (Anedda et al., 2023). Therefore, there is a need to better identify the hepatic liabilities in response to a new insect protein.

The use and validation of fish hepatic health monitoring tools have become increasingly evident due to the expansion of aquaculture. The assessment of liver damage encompasses the evaluation of liver function markers, such as histopathologic and ultrastructure changes, as well as variations in indices pertaining to liver function, liver lipid and glycogen content, antioxidant biomarkers, inflammatory and apoptotic factors, serum hepatic enzymes, and other relevant parameters. It can be used to monitor the health status of fish in response to changes related to feed ingredients. The ability of the liver to sense protein in carnivorous fish has been partially evaluated to date. We have evaluated the expression of markers involved in the detection of plant protein in the liver of the strictly carnivorous fish species largemouth bass (*Micropterus salmoides*) in response to an oral cottonseed protein concentrate (He et al., 2022). These markers included the histopathology, antioxidant enzymes (superoxide dismutase [SOD], catalase [CAT] and glutathione peroxidase [GPX]) and genes (*sod, cat, gshpx*), inflammatory cytokines, and protein metabolism genes (*P13K*, *AKT*, *mTOR*, *S6K1*), which were considered suitable as a predictor for the health status of fish in response to changes related to nutrition.

Numerous research investigations have been dedicated to exploring the substitution of fish meal with alternative protein sources. Nevertheless, there is currently limited understanding regarding the molecular mechanisms underlying the utilization of diets containing diverse protein sources in fish. The body weight and weight gain rate (WGR) decreased when the fish were fed diets with 10%, 15%, and 20% *H. illucens* instead of fishmeal in largemouth bass. However, the hepatic and intestinal histomorphology of all the fish was unaffected (Wang et al., 2022). Therefore, we designed the experiment in which largemouth bass were fed different diet proportions of HI instead of fishmeal at 0%, 20%, and 40% HI for 80 d. To uncover the relationship between gene expression and utilization of insect protein, transcriptomic and metabolomic techniques were performed. The omics were employed to elucidate the differentially expressed genes (DEG), changed secondary metabolites, and enriched pathways in juvenile largemouth bass in response to *H. illucens* meal. This analysis ultimately unveiled the underlying response mechanisms, facilitating the exploration of protein sources and enhancing the production performance of fish.

2. Materials and methods

2.1. Animal ethics statement

The experimental design and procedure in this study were approved by the Animal Ethics Committee of Southwest University (No. IACUC-20181015-12, 15 October 2018, China). All animal experiments complied with the ARRIVE guidelines.

2.2. Feed preparation

Black soldier fly larvae (*H. illucens* L.) were purchased from Chongqing BaMu Agricultural Technology Co., Ltd., Chongqing, China. The *H. illucens* were dried at 70 °C for 30 min and subsequently air dried. Finally, the dried larvae were crushed to powder through a 1.0-mm mesh, and then kept in a well-closed and light resistant place.

Three isoproteic and isolipidic diets were formulated to replace 0% (HI0, control), 20% (HI20), 40% (HI40) of fish meal by a corresponding amount of *H. illucens* (Table 1). The test diets were supplemented with a combination of L-lysine·H_2SO_4 and DL-methionine hydroxy analogue calcium (MHA-Ca) to match the essential amino acid (EAA) and fatty acid (FA) profiles of the control diet, respectively. The dry matter in the basal diet was formulated to contain crude protein at approximately 48% and crude lipid at approximately 14%, which were measured by the Kjeldahl method and the Soxhlet exhaustive extraction technique, respectively,

Table 1
Composition of the trial diets (dry matter, %).

Item	Groups[1]		
	HI0 (control)	HI20	HI40
Ingredients			
Fish meal	35.00	28.00	21.00
Chicken meal	15.00	15.00	15.00
H. illucens	0.00	11.90	23.80
Soybean meal	7.00	7.00	7.00
Soy protein concentrate	6.00	6.00	6.00
Concentrated cottonseed protein	5.00	5.00	5.00
Wheat gluten	3.00	3.00	3.00
Cassava starch	9.00	9.00	9.00
Fish oil	3.00	1.52	0.03
Soybean lecithin	1.00	1.00	1.00
Soybean oil	5.00	2.53	0.05
Vitamin premix[2]	1.50	1.50	1.50
Mineral premix[3]	1.50	1.50	1.50
Choline chloride	0.50	0.50	0.50
Calcium dihydrogen phosphate	1.50	1.50	1.50
Vitamin C	0.05	0.05	0.05
Ethoxyquin	0.05	0.05	0.05
Microcrystalline cellulose	5.90	4.83	3.75
Lys	0.00	0.07	0.15
Met	0.00	0.06	0.12
Nutrients levels[4]			
Crude protein	47.94	47.87	47.51
Crude lipid	14.02	13.91	14.23
Ash	12.25	11.82	11.48
Gross energy[5], MJ/kg	18.14	18.19	18.32

[1] HI0: 0% of fish meal substituted by *H. illucens* meal; HI20: 20% of fish meal substituted by *H. illucens* meal; HI40: 40% of fish meal substituted by *H. illucens* meal.
[2] Vitamin premix (mg/kg of diet): vitamin A, 9; vitamin D_3, 2.5; vitamin E, 75; vitamin C (350 g/kg), 250; vitamin B_1, 8; vitamin B_6, 10; vitamin B_{12}, 3; vitamin K_3, 9; riboflavin, 20; inositol, 160; calcium-D-pantothenate, 30; niacinamide, 40; folic acid, 2.5; biotin, 1; ethoxyquin, 50.
[3] Mineral premix (mg/kg of diet): Na, 15; K, 25; Mg, 50; Cu, 2; Fe, 12.5; Zn, 17.5; Mn, 6; I, 0.8; Se, 0.1; Co, 0.4.
[4] Crude protein and crude lipid were measured value.
[5] Gross energy was calculated by NRC (2007) contents.

using the standard methodology (AOAC, 2005; Jiang et al., 2014; Manirakiza et al., 2001). All ingredients were ground through a 177-μm mesh before final mixing and then blended with the oil. The experimental diets were prepared using a dry power press MUZL180 (Muyang Group, Jiangsu, China), then air dried and stored at 4 °C until use.

2.3. Feeding trial

Largemouth bass (*M. salmoides*) were obtained from a commercial farm (Changshou, Chongqing, China). Before the trial, the fish were acclimated and provided with a commercial feed (Guangzhou Haida Feed Co., Ltd, China) for a duration of 7 d.

At the start of the experiment, the fish were fasted for 24 h and weighed after being anesthetized with 0.1 g/kg MS-222 (Sigma, USA). Largemouth bass (mean initial weight = 10.02 ± 0.03 g) were randomly allocated into 9 cylindrical plastic tanks (capacity = 300 L) with screened covers for the growth trial (30 fish per tank). Each dietary treatment group was randomly assigned to three tanks. The fish were acclimated and provided with commercial feed, the proportion of which was gradually reduced over a period of 7 d until they adapted. Fish were fed to apparent satiation by hand two times (08:30, 18:30) daily for 80 d. During the experimental period, the water temperature ranged from 26 to 31 °C, dissolved oxygen content was kept at 6.8 to 7.2 mg/L, pH 7.0 to 7.2, and NH_4^+–N < 0.6 mg/L. The photoperiod was 12L:12D, with the light period from 08:00 to 20:00.

2.4. Sample collection

On the 80th day of the experiment, 6 h after the last feeding, 9 animals per treatment group (3 fish per replicate) were randomly selected and anesthetized with 0.1 g/L MS-222 (Sigma, USA). The liver was collected for enzyme analysis, immediately frozen in liquid nitrogen, and stored at −80 °C for further analysis. Meanwhile, another 18 animals per treatment group (6 fish per replicate) were individually used for collecting the liver tissue for RNA isolation, and samples with the protector (RNA/DNA, TaKaRa, Type 9750, Tokyo, Japan) were fast frozen in liquid nitrogen. Subsequently, at postprandial 24 h, 15 animals per treatment group (5 fish per tank) were individually used for determining the morphological parameters, body composition and for collecting liver tissue for their histology assays. The liver samples (the central part of the liver, approximately 1 cm^3) were fixed in 4% paraformaldehyde for histology determination, and stored at room temperature until analysis. At the end of the experiment, all the fish were counted and weighed.

2.5. Chemical analysis

All chemical composition analysis of diets were conducted by standard methods (AOAC, 2005). Moisture content was determined by oven drying to a constant weight at 105 °C in DHG-9240A (Keelrein Instrument Co. Ltd., China). Protein content was determined by measuring nitrogen (N × 6.25) using the Kjeldahl method in FOSS Kjeltec2300 (Foss Analytical Instruments Co. Ltd., Sweden); lipid by ether extraction (without acid hydrolysis) using Soxtec; ash content by combustion at 550 °C for 12 h in a muffle furnace (Shenyang Energy- Saving Electric Furnace Factory, China).

The activities of SOD, CAT, GSH-Px, and malondialdehyde (MDA) content in liver were assayed with commercial kits (Nanjing Jiancheng Bioengineering Institute, Nanjing, China). All quantitative assays were performed in triplicate.

2.6. Morphological analysis

The liver samples were stained with hematoxylin and eosin (H&E) and oil red O, which were fixed in 4% paraformaldehyde solution (Servicebio, G1101) for at least 24 h, dehydrated in graded ethanol concentrations and embedded in paraffin wax. Serial sections were cut to 5 μm thickness and mounted on glass slides. Sections were deparaffinized in xylene, hydrated in ethanol and stained with H&E or oil red O. Subsequently, the morphology was observed under a light microscope (OLYMPUS, DP73, Nikon Corporation, Japan).

2.7. RNA extraction and quantitative real-time PCR

Total RNA was extracted from the liver using the RNAiso Plus reagent (TaKaRa, Shiga, Japan) and quantified using a NanoDrop 2000 (Thermo Fisher Scientific, USA). Complementary DNA (cDNA) was synthesized from RNA with an NovoScript Plus All-in-one 1st Strand cDNA Synthesis Mix (TaKaRa, Shiga, Japan), and stored at −20 °C. Primer sequences used for PCR were synthesized by Beijing Qingke Biotech Co., Ltd., China (Table S1). Quantitative real time PCR was performed using a CFX96TM Real-Time System (Bio-Rad, USA). HI0 was the control group and HI20 and HI40 were the experimental groups ($n = 6$). Reaction system refers to the TB Green Premix Ex Taq instructions provided by the manufacturer (repeats: 3) as follows: 95 °C pre-denaturation for 30 s, 39 cycles of denaturation at 95 °C for 5 s, annealing and extension at 60 °C for 30 s, and finally, melt curve analysis (TaKaRa, Shiga, Japan). With β-actin used as reference gene, relative quantification of gene expression was analyzed by the $2^{-\triangle\triangle Ct}$ method (Livak and Schmittgen, 2001) and the results expressed as the extent of change with respect to control values.

2.8. RNA-Seq and data analysis

Total RNA samples extracted from liver of fish from the HI0 and HI40 groups were subjected to RNA-Seq. Sequencing library construction and high throughput sequencing were performed by the ICONGENE Gene Technology Co., Ltd (Wuhan, China) with conventional Illumina protocols. Three replicates for each experimental group were involved in the analysis. The libraries were sequenced with 150-bp paired-end reads. The raw RNA-seq reads were deposited in the NCBI Sequence Read Archive (SRA) under the BioProject accession number PRJNA998590.

The raw sequencing reads were preprocessed and filtered using fastp (0.23.2) (Chen et al., 2018). The clean reads were mapped to the reference genomic sequence database (ASM1485139v1, downloaded from NCBI) of largemouth bass using hisat2 (2.2.1) (Kim et al., 2019) with default parameters. The mapped reads were assigned to the genes using featureCounts, a tool of subread (2.0.3) (Liao et al., 2014). Gene abundance was calculated as fragments per kilobase of transcript per million fragments mapped (FPKM). Genes with FPKM ≥0.1 in all samples of at least one sample group were regarded as expressed. Only the expressed genes were subjected to subsequent analyses. The differentially expressed genes (DEG) between the control and treatment groups were identified by DESeq2 (1.40.2) (Love et al., 2014). The thresholds for identification of DEG were fold change ≥1.5 and adjusted *P*-value <0.05. Principal component analysis (PCA) was conducted using Arraytrack (Fang et al., 2017). Hierarchical clustering analysis for the gene expression data was performed by GENE-E (https://software.broadinstitute.org/GENE-E/). To find the zebrafish homologs of the largemouth bass genes, the largemouth bass transcripts were used to search the zebrafish proteome by blastx (2.13.0) (Sayers et al., 2022). Gene Ontology (GO) and Kyoto Encyclopedia of

Genes and Genomes (KEGG) enrichments for the DEG were identified by ClueGO (Bindea et al., 2009) using the zebrafish annotation file and list of the expressed genes was used as the reference for enrichment analysis.

2.9. Metabolomic assay and data analysis

Metabolomic analysis for the liver samples of the individuals from the HI0 and HI40 groups were conducted by the Biomarker Technologies (Beijing, China). Three replicates were involved for each treatment group. The samples were homogenized and metabolites were extracted using a mixture of methanol and acetonitrile (1:1). The samples were centrifuged and the supernatant was collected into new tubes. The extracts were dried by evaporation and dissolved in an acetonitrile water solution (1:1).

Mass analysis was conducted using a LC/MS system comprised of a Waters Acquity I-Class PLUS ultra-high performance liquid tandem Waters Xevo G2-XS QT of high-resolution mass spectrometer. An ACQUITY UPLC HSS T3 (2.1 mm × 100 mm, 1.8 μm) column (Waters Corporation, USA) were used. The solvents for the positive ion mode were mobile phase A: 0.1% formic acid aqueous solution, mobile phase B: 0.1% formic acid acetonitrile; while those for the negative ion mode were mobile phase A: 0.1% formic acid aqueous solution, mobile phase B: 0.1% formic acid acetonitrile. The injection volume was 1 μL. The primary and secondary mass spectrometry data in MSe mode were collected by the MassLynx acquisition software (V4.2, Waters). In each data acquisition cycle, dual-channel data acquisition was performed with both low and high collision energy at the same time. The low collision energy was 2 V, the high collision energy range was 10 to 40 V, and the scanning frequency was 0.2 s for a mass spectrum. The parameters of the ESI ion source were as follows: capillary voltage 2000 V for the positive ion mode and −1500 V for the negative ion mode, cone voltage 30 V, ion source temperature 150 °C, desolvent gas temperature 500 °C, backflush gas flow rate 50 L/h, desolventizing gas flow rate 800 L/h. The raw data collected by MassLynx (V4.2) was processed by Progenesis QI software (Waters) for peak extraction, peak alignment and other data processing operations. Compound identification was based on the METLIN online database and Biomarker's self-built library. Mass deviation was within 100 mg/L.

The identified compounds were annotated by searching the KEGG, HMDB and LIPID MAPS databases. Orthogonal partial least square discriminant analysis (OPLS-DA) was performed using the ropls (1.32.0) (Thevenot et al., 2015). Compound ID conversion and pathway analysis were conducted by MetaboAnalyst (5.0) (Pang et al., 2021). The threshold for differential metabolite was $P < 0.05$. The differential genes and metabolites were subjected to joint-pathway analysis. A network for the differential genes and metabolites in the pathways associated with amino acid biosynthesis and metabolism was generated and visualized using Cytoscape (V3.10.0) (Shannon et al., 2003).

2.10. Statistical analysis

All the data were expressed as mean ± standard deviation and the results were analyzed by one- way ANOVA followed by Tukey's analysis using SPSS Statistics version 20.0 statistical program. A value of $P < 0.05$ was considered as statistically significant.

3. Results

3.1. Growth performance

The growth performance of fish fed on diets supplemented with different level of HI meal is presented in Table 2. No significant difference in survival rate was found among the experimental groups ($P > 0.05$). The fish fed with the HI40 diet had significantly lower ($P < 0.05$) WGR, SGR and PER, and significantly higher ($P < 0.05$) FCR compared to the fish of the HI0 and HI20 groups.

Table 2
Effects of *H. illucens* on growth performance and feed utilization of largemouth bass.[1]

Item	Groups		
	HI0 (control)	HI20	HI40
Initial body weight, g/fish	10.01 ± 0.02	10.02 ± 0.04	10.03 ± 0.01
Final body weight, g/fish	83.46 ± 0.14[a]	85.04 ± 0.16[a]	72.69 ± 1.10[b]
WGR[2], %	734.62 ± 3.00[a]	749.08 ± 0.37[a]	624.87 ± 11.47[b]
SGR[3], %/day	2.65 ± 0.01[a]	2.67 ± 0.00[a]	2.48 ± 0.02[b]
FI[4], g/fish	2.16 ± 0.01[b]	2.13 ± 0.01[b]	2.31 ± 0.04[a]
FCR[5]	1.10 ± 0.01[b]	1.08 ± 0.00[b]	1.24 ± 0.03[a]
PER[6]	1.89 ± 0.01[a]	1.93 ± 0.01[a]	1.69 ± 0.04[b]
SR[7], %	100.00 ± 0.00	100.00 ± 0.00	100.00 ± 0.00

[1] HI0: 0% of fish meal substituted by *H. illucens* meal; HI20: 20% of fish meal substituted by *H. illucens* meal; HI40: 40% of fish meal substituted by *H. illucens* meal. Data presented as mean ± SD, $n = 3$. Different letters in each row indicate significant difference between the means by Tukey's test ($P < 0.05$).
[2] Weight gain rate (WGR) = [final weight (g) − initial weight (g)] × 100/initial weight (g).
[3] Specific growth rate (SGR) = [ln (mean final weight) − ln (mean initial weight)/80 (d)] × 100.
[4] Feed intake (FI) = feed consumption (g)/[(initial weight + final weight)/2 × 80 (d)]. This is daily feed intake in relation to body weight.
[5] Protein efficiency ratio (PER) = total weight gain (g)/protein intake (g).
[6] Feed conversion ratio (FCR) = total feed intake in dry basis (g)/weight gain (g).
[7] Survival rate = 100 × (final number − initial number)/initial number.

3.2. Hepatic histological changes

The livers of fish belonging to different experimental groups were checked immediately after being dissected. The control fish had normal reddish-brown livers and HI20 group had reddish-yellow livers, while those from the HI40 group had yellowing livers (Fig. 1). Moreover, high dietary HI meal (HI40) resulted in irregular hepatic cord arrangement (Fig. 1, indicated by the green arrow). Compared with the control group, the H&E-stained sections revealed that the liver tissue of the HI20 and HI40-fish groups showed increased intracellular vacuolization (Fig. 1, indicated by the yellow arrow), more condensed nuclei (Fig. 1, indicated by the blue arrow) and cells with fractured or even completely disappeared nuclei. The pathological symptoms were more pronounced in the HI40-fish group. The results of oil red O staining demonstrated that the liver tissue of the HI40-fish accumulated more neutral lipid droplets in the cells (Fig. 1, indicated by the red arrows). Together, substituting 40% of fishmeal in the feed with HI meal changed the morphology, tissue structure and increased lipid accumulation in the liver of largemouth bass.

3.3. Feeding a high HI meal diet caused oxidative stress in the liver

Activities of the antioxidative enzymes including SOD, GSH-Px and CAT were characterized to assess the effects of high dietary HI meal on antioxidative ability of the liver. As shown in Table 3, while no significant difference in the activity of GSH-Px was identified ($P > 0.05$), the HI40 group had significantly lower ($P < 0.05$) CAT and SOD activities compared to the control and HI20 groups. Consistent with the decreased activities of the antioxidative enzymes, MDA content of the HI40 samples was significantly higher ($P < 0.05$) than those of the control and HI20 samples (Table 3). In summary, feeding a high HI meal diet decreased activities of the antioxidative enzymes and increased the content of lipid oxidation product.

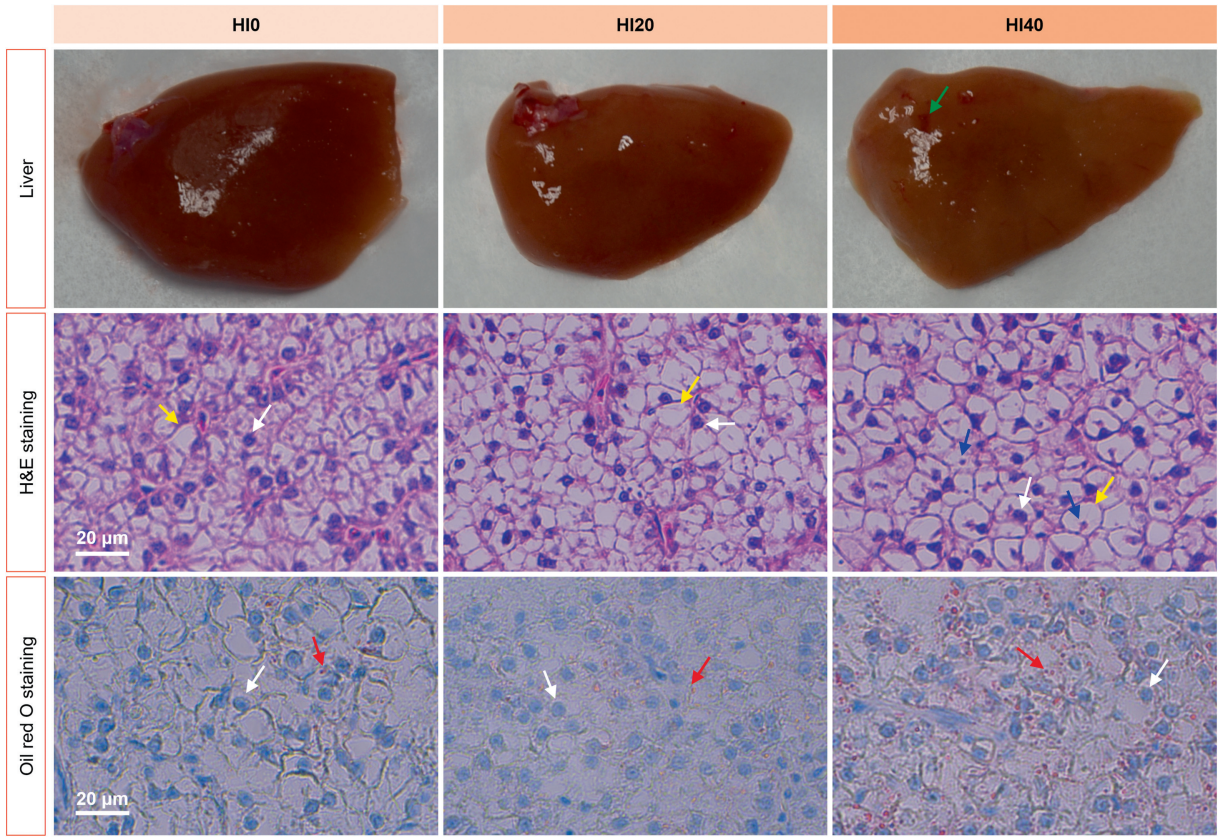

Fig. 1. Representative photos of liver and hematoxylin and eosin (H&E)- and oil red O-stained liver sections. HI0: 0% of fish meal substituted by *H. illucens* meal; HI20: 20% of fish meal substituted by *H. illucens* meal; HI40: 40% of fish meal substituted by *H. illucens* meal. The green, yellow and red arrows indicate hepatic cord, liver vacuoles, and lipid droplets, respectively; the white and blue arrows indicate normal and condensed nuclei.

Table 3
Oxidative indices including SOD, GSH-Px, and CAT activities and MDA content.[1]

Item	HI0 (control)	HI20	HI40
SOD, U/mg prot	405.97 ± 15.65[a]	401.74 ± 3.43[a]	357.75 ± 5.96[b]
GSH-Px, U/mg prot	25.71 ± 0.56	24.18 ± 1.78	23.10 ± 0.71
CAT, U/mg prot	8.78 ± 0.01[a]	8.73 ± 0.40[a]	6.42 ± 0.15[b]
MDA, pmol/mg prot	8.96 ± 0.03[b]	9.06 ± 0.25[b]	10.99 ± 0.22[a]

SOD = superoxide dismutase; CAT = catalase, GSH-Px = glutathione peroxidase, MDA = malondialdehyde.
Data are expressed as means ± SD (n = 3). Different letters in each row indicate significant difference between the means by Tukey's test ($P < 0.05$).
[1] HI0: 0% of fish meal substituted by *H. illucens* meal; HI20: 20% of fish meal substituted by *H. illucens* meal; HI40: 40% of fish meal substituted by *H. illucens* meal.

3.4. Biological processes affected by high dietary HI meal

The effects of high dietary HI on liver transcriptome were explored by RNA-Seq. The RNA-Seq reads statistics are shown in Table S4 and the results of principal component analysis (PCA) for the gene transcriptional expression data demonstrated that HI0 and HI40 samples were clearly separated (Fig. 2A), indicating significant deviation in gene expression. The genes differentially expressed between the HI40 and HI0 samples were identified (Fig. 2B). In total, 344 upregulated and 256 downregulated genes were identified. To validate the RNA-seq data, the expressions of 13 genes were analyzed by qPCR. Significant correlation ($P < 0.001$, Fig. S1) was found between the qPCR and RNA-seq data. The *fmo5*, *hhex*, and *aqp12* genes were the top upregulated genes, while *rmdn3*, *per1b* and *gas1b* were the top downregulated genes (Fig. 2C).

GO enrichment analyses were performed for the differentially expressed genes to investigate the biological processes affected by high dietary HI. The full lists of the GO enriched among the up and downregulated genes are shown in Table S2. The upregulated genes were enriched in biological processes aimed at protein synthesis, such as RNA processing, ribosome biogenesis and regulation of translation, indicating enhanced protein synthesis in the liver cells (Fig. 2D). Furthermore, biological processes associated with protein catabolism, such as proteasomal protein catabolic process and ubiquitin-dependent ERAD pathway, were also overrepresented by the upregulated genes (Fig. 2D and Table S2). The simultaneous enrichment of protein biosynthesis and catabolic processes suggested an enhanced protein turnover rate. Moreover, enrichment of the upregulated genes in response to endoplasmic reticulum stress (Fig. 2D) indicated the induction of endoplasmic reticulum (ER) stress. Together, these results indicated that high dietary HI meal may induce ER stress and disturbed the homeostasis of protein metabolism in the liver of largemouth bass.

The downregulated genes were enriched in biological processes such as regulation of cell population proliferation, regulation of circadian rhythm, lymphocyte differentiation and autophagosome assembly (Fig. 2E and Table S2). These processes were associated with cellular proliferation, growth, metabolism, immunity and maintenance of tissue homeostasis. Downregulation of the genes involved in these processes is consistent with the decreased growth performance and impaired health of the fish in the HI40 group. Furthermore, regulation of phosphatidylinositol 3-kinase activity,

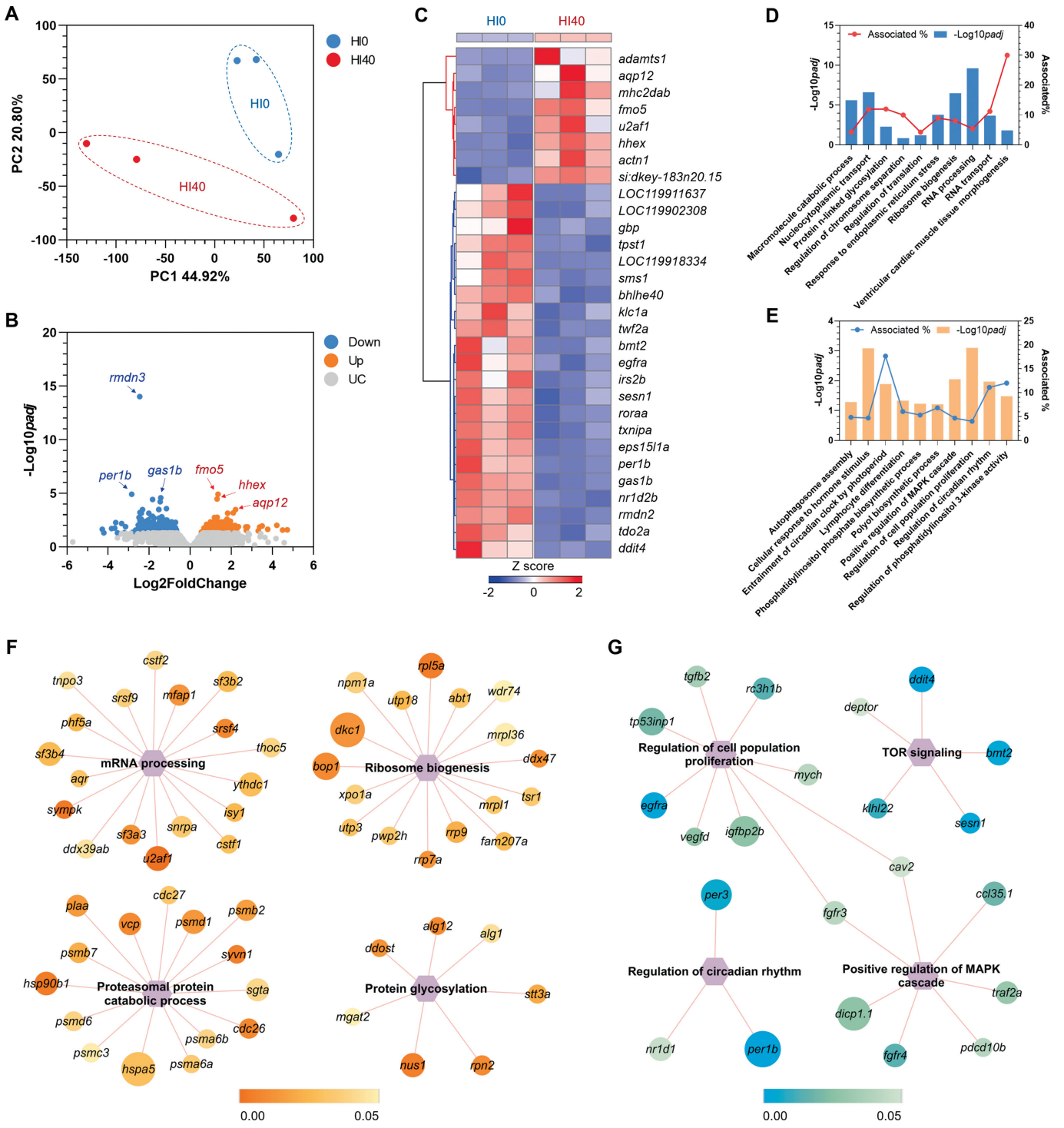

Fig. 2. Overall genes expression and results of Gene Ontology (GO) enrichment analysis. HI0: 0% of fish meal substituted by *H. illucens* meal; HI40: 40% of fish meal substituted by *H. illucens* meal. (A) A scatter plot demonstrating the results of principal component analysis (PCA) for the gene expression data. The dashed circles indicate distribution of the sample groups (HI0 and HI40) in the PCA plain. (B) A volcano plot indicating the differentially expressed genes (DEG). The top up- and down-regulated genes are shown. (C) A heatmap indicating expression profiles of the top 30 DEG. (D and E) Top GO enrichments for the upregulated (D) and downregulated genes (E). (F and G) DEG associated with the representative biological processes enriched among the upregulated (F) and downregulated genes (G). Only the genes had a log2 fold change value ≥ 1 or ≤ -1 were included. Size of the nodes is proportional to the absolute log2 fold change values. The color scales indicate adjusted *P*-value of the genes.

positive regulation of mitogen-activated protein kinase (MAPK) cascade and regulation of target of rapamycin (TOR) signaling were also enriched among the downregulated genes (Table S2).

The DEG involved in the representative biological processes are also displayed. For instance, *u2af1*, *sympk*, and *srsf4* are the top upregulated genes involved in mRNA processing (Fig. 2F); while

egrfa, *igfbp2b*, and *rc3h1b* are the top downregulated genes involved in regulation of cell population proliferation (Fig. 2G).

3.5. Biological pathways impacted by high dietary HI meal

The upregulated genes were highly enriched in the KEGG pathways such as protein processing in the endoplasmic reticulum, spliceosome and nucleocytoplasmic transport, ribosome biogenesis in eukaryotes and N-glycan biosynthesis (Fig. 3A, Table S3). These pathways were mainly associated with protein biosynthesis, processing and modification. The downregulated genes were enriched in the adipocytokine signaling, p53 signaling, RIG-I-like receptor signaling pathways and intestinal immune network for immunoglobulin A production (Fig. 3B, Table S3). These pathways were involved in cell survival and immune responses.

The DEG associated with the representative pathways are also shown. For example, *pdia6*, *hsp90b1* and *pdia4* were top upregulated genes involved in protein processing in the endoplasmic reticulum (Fig. 3C); while *traf2a*, *ikbkg*, and *cxcl19* were the top downregulated genes associated with the RIG-I receptor signaling pathway (Fig. 3D).

3.6. Effects of high dietary HI meal on liver metabolome

Metabolomic analysis was conducted to investigate the effect of high dietary HI. In total, 5915 metabolites were identified, including 3715 and 2200 metabolites identified by the positive and negative modes respectively. Abundance data of the positive and negative metabolites were combined and subjected to the subsequent analyses. The results OPLS-DA indicated that samples of the same treatment groups clustered together and the differences in metabolite abundance between the HI0 and HI40 groups were projected to component 1 (Fig. 4A).

The HI40 samples had 451 upregulated and 681 downregulated metabolites compared to the controls. The most significantly up- and down-regulated compounds in the HI40 samples were 2″-(6-acetylglucosyl)astragalin and 1-(2-furanylmethyl)-1h-pyrrole (Fig. 4B). Profiles of the top 30 differential metabolites as a result of high dietary HI are shown. Among these top differential metabolites, 13 were increased and 17 were decreased (Fig. 4C).

The results of pathway enrichment analysis indicated that pathways including one carbon pool by folate, propanoate metabolism, alpha-linolenic acid metabolism, linoleic acid metabolism, folate biosynthesis and tryptophan metabolism were significantly ($P < 0.05$) enriched among the differential metabolites (Fig. 4D). A joint transcriptomic–metabolomic pathway analysis revealed that ascorbate and aldarate metabolism, one carbon pool by folate, linoleic acid metabolism, drug metabolism – other enzymes and alpha-linolenic acid metabolism were the pathways over-represented ($P < 0.10$) by the differential genes and metabolites (Fig. 4E).

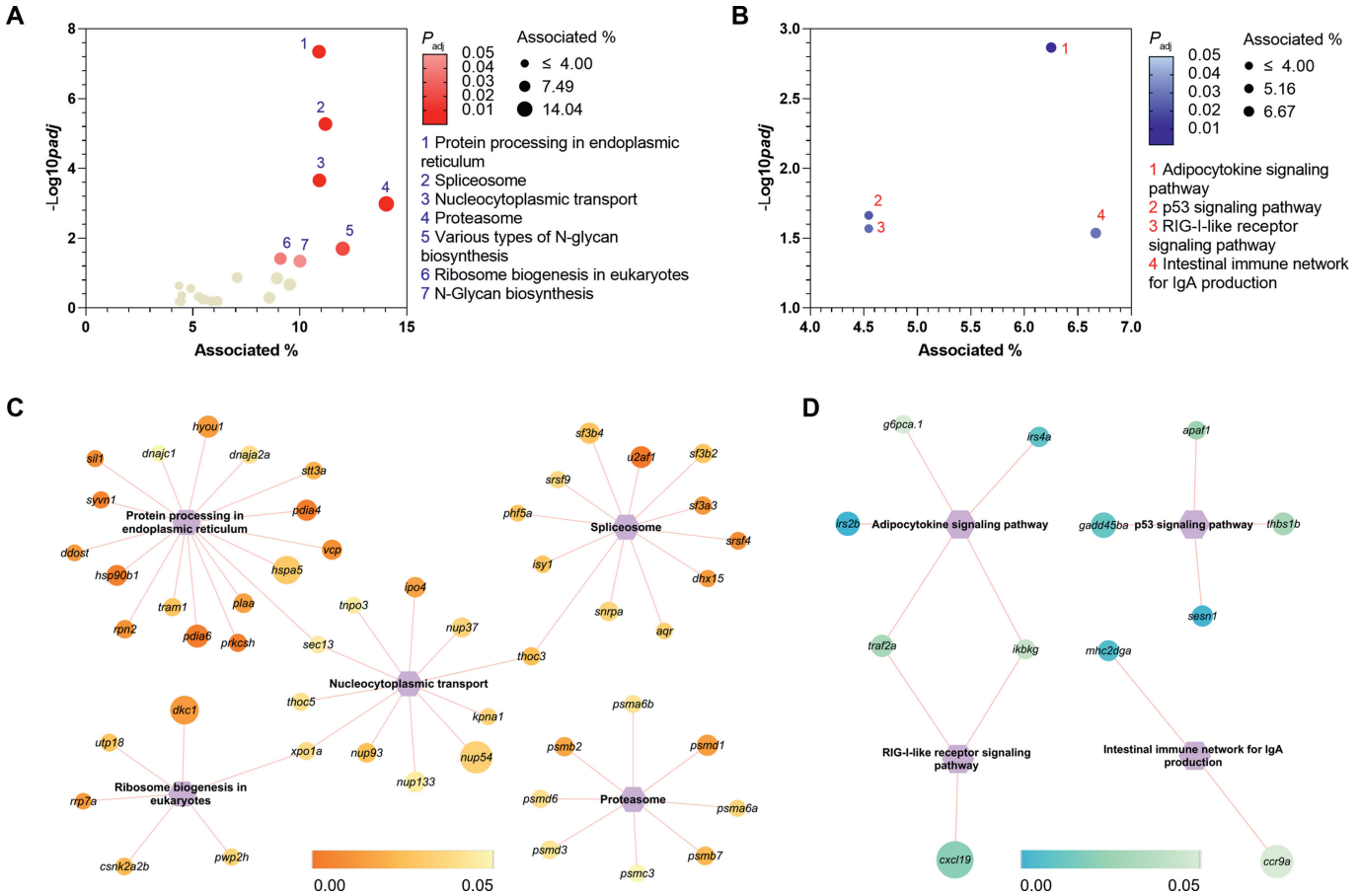

Fig. 3. Results of KEGG pathway enrichment analysis. (A and B) KEGG pathway enrichments for the upregulated (A) and downregulated genes (B). *Padj*, corrected *P* value; Associated %, percentage of genes associated with the enriched terms. (C and D) DEG associated with the representative KEGG pathways enriched among the upregulated (C) and downregulated genes (D). Only the genes had a log2 fold change value ≥ 1 or ≤ −1 were included. Size of the nodes is proportional to the absolute log2 fold change values. The color scales indicate adjusted *P*-value of the genes. KEGG = Kyoto Encyclopedia of Genes and Genomes; DEG= differentially expressed genes.

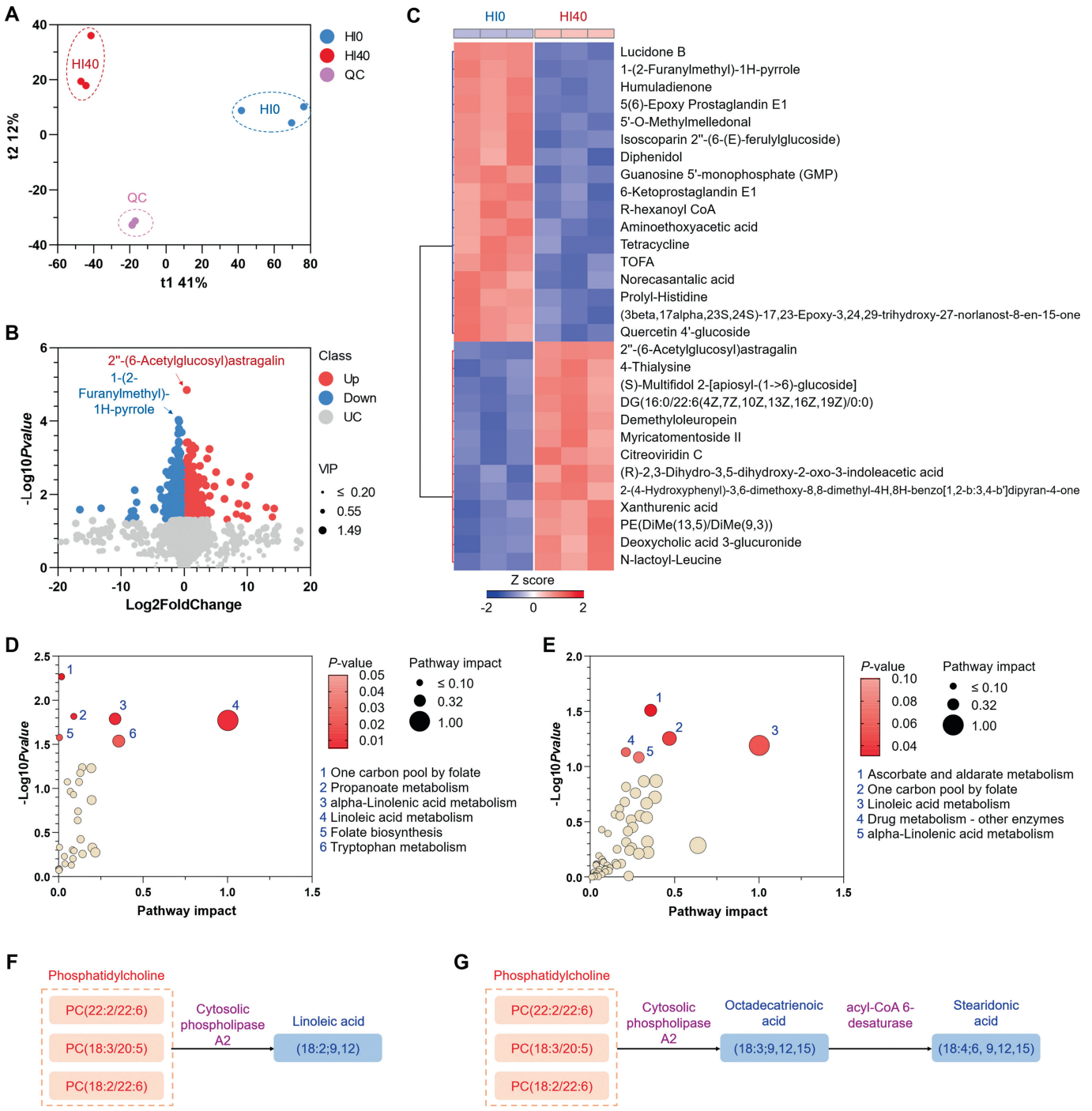

Fig. 4. Changes in liver metabolome caused by high dietary *H. illucens* meal. HI0: 0% of fish meal substituted by *H. illucens* meal; HI40: 40% of fish meal substituted by *H. illucens* meal. (A) A scatter plot indicating results of the orthogonal partial least squares discriminant analysis (OPLS-DA) for the metabolomic data. The dashed circles indicate distribution of the sample groups (HI0 and HI40). (B) A volcano plot demonstrating the differential metabolites. The top up and downregulated metabolites are shown. (C) A heatmap indicating abundance profiles of the top 30 differential metabolites. (D) KEGG pathway enrichments for the differential metabolites. (E) KEGG pathway enrichments identified by joint-pathway analysis. (F and G) Differential metabolites in the linoleic acid metabolism (F) and alpha-linolenic acid metabolism pathways (G). The increased and decreased metabolites are shown in red and blue, respectively. The enzymes catalyze the reactions are shown in purple. The arrows indicate reaction direction from substrates to products. KEGG = Kyoto Encyclopedia of Genes and Genomes; PC = phosphatidylcholine.

In the linolenic acid metabolism and alpha-linolenic acid metabolism pathways, the contents of linoleic acid (18:2;9,12; Fig. 4F), and octadecatrienoic acid (18:3;9,12,15) and stearidonic acid (18:4;6,9,12,15; Fig. 4G) were significantly decreased in the HI40 samples compared to the controls. The substrates and the enzymes that catalyze the reactions are also shown.

Furthermore, we generated a network for the differential genes and metabolites that were associated with amino acid biosynthesis and metabolism to understand the effects of high dietary HI meal on amino acid metabolism (Fig. 5). The differential genes and metabolites were distributed into 10 amino acid metabolism pathways. Tryptophan, arginine and proline metabolism contained the

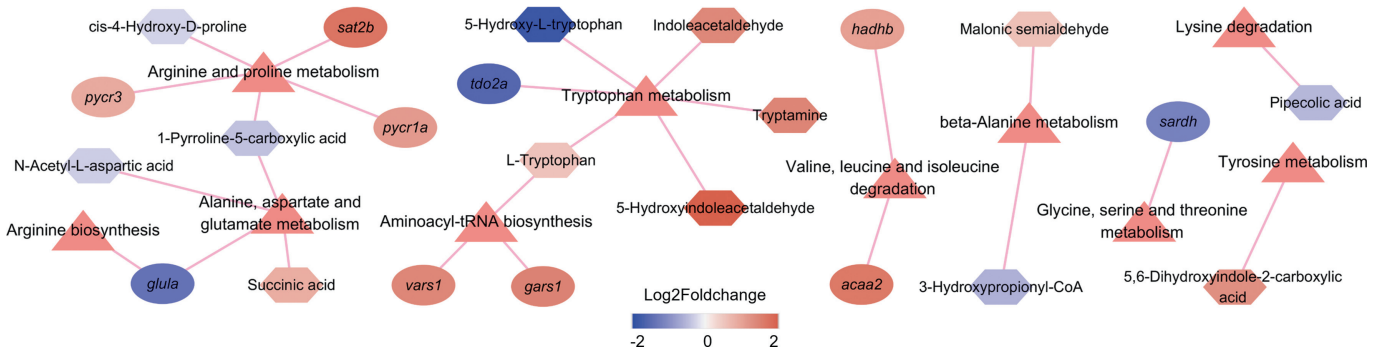

Fig. 5. A network for the differential genes and metabolites associated with the amino acid biosynthesis and metabolism pathways. The nodes represent pathways (the triangles), genes (the circles) and metabolites (the hexagons). The edges (the lines) stand for involvement of the genes and metabolites in the corresponding pathways. The color scale indicates Log2 fold change for the genes and metabolites.

largest number of differential genes and metabolites, suggesting that these pathways are likely to be affected by high HI substitution. For example, the tryptophan 2,3-dioxygenase a (*tdo2a*) gene and 5-hydroxy-tryptophan were highly downregulated in the HI40 samples compared to the controls. The glutamate-ammonia ligase (glutamine synthase) a (*glula*) gene involved in arginine biosynthesis and alanine, aspartate and glutamate metabolism, and the sarcosine dehydrogenase (*sardh*) gene involved in glycine, serine and threonine metabolism were also significantly downregulated in the HI40 samples (Fig. 5). Together, alteration in abundance of these genes and metabolites may account for the adverse effects of high dietary HI on fish growth.

4. Discussion

It is imperative for the aquaculture industry to find substitutes for fishmeal in the feeds of farmed fishes due to decreasing natural resources and the increasing price of fishmeal. HI meal has been previously used to partially replace fishmeal in the feeds of fish species including gilthead seabream (*Sparus aurata*) (Bosi et al., 2021; Randazzo et al., 2021), rainbow trout (*Oncorhynchus mykiss*) (Rimoldi et al., 2019), tongue sole (*Cynoglossus semilaevis*) (Li et al., 2022) and zebrafish (*Danio rerio*) (Fronte et al., 2021). The effects of replacing fishmeal with HI meal depend on fish species and the amount of substitution. For example, no adverse effects on growth performance and histological traits were observed in zebrafish when HI meal was included up to 20% in the diet and even when replacing 100% of the fishmeal (Fronte et al., 2021). Replacing 40% of dietary fishmeal with HI meal significantly improved growth rate of gilthead seabream (Randazzo et al., 2021). Inclusion of HI meal (up to 30%) in the diets of rainbow trout was reported to improve fish health through influencing the intestinal bacterial community (Rimoldi et al., 2019). In tongue sole (*C. semilaevis*), low-level (substituting 25% of fishmeal) dietary HI meal had positive effects on growth; however, the substitution of fishmeal up to 50% resulted in a significant decrease in growth, intestinal structural damage and abnormal liver function (Li et al., 2022).

Although adverse effects of high dietary HI meal on fish growth and health were previously reported, the underlying molecular mechanisms remain unknown. In this study, the molecular basis of high dietary HI meal was investigated using a multi-omics approach to integrate transcriptomics and metabolomics associated with differences in largemouth bass. Although three samples were too few for omics analysis, they did convey some noteworthy messages and provided new insights for future research. The transcriptomic data reveal that feeding on a high HI meal diet induced expression of the genes responsible for protein synthesis, proteolysis, protein localization and transport, suggesting an enhanced protein turnover rate. Similar to the present study, enrichment of protein synthesis and catabolic processes were found in other omics studies in less feed efficient chinook salmon (*Oncorhynchus tshawytscha*) (Esmaeili et al., 2022, 2023). Enhanced protein synthesis and degradation are energy demanding for the cells, which may disturb physiological functions of the liver. Furthermore, the genes involved in response to endoplasmic reticulum (ER) stress, such as *hspa5* and *hsp90b1* were also induced in the liver of the fish fed on a high HI meal diet. The increase in proteins and transcripts involved in protein processing in the ER and proteolysis has been previously reported in less feed efficient chinook salmon (Esmaeili et al., 2021). Endoplasmic reticulum stress was postulated to be triggered by a nutritional deficiency and was regarded as a key mechanism in the stunted growth of seawater rainbow trout (Morro et al., 2021). It was previously reported that feeding juvenile largemouth bass with a high carbohydrate diet also induced ER stress and oxidative stress in the intestine (Zhao et al., 2021). Similar to the results of our study, low dietary fishmeal induced ER stress in juvenile pacific white shrimp (*Litopenaeus vannamei*) (Xie et al., 2020). These results indicate that the unbalanced nutritional composition of the diets can inhibit growth of farmed species by inducing ER stress.

In addition, the upregulated genes in the liver of the HI40 fish are significantly enriched in processes and pathways for protein glycosylation. N-glycosylation is a highly conserved protein post-translation modification and it was reported that more than 7000 human proteins are N-glycosylated (Hirata and Kizuka, 2021). N-glycosylation is critical for protein function, which affects protein folding, trafficking, stability and interaction (Esmail and Manolson, 2021). The N-glycan precursor is synthesized in the ER (Hirata and Kizuka, 2021). Considering the induction of genes involved in ER stress, upregulation of genes involved in N-glycosylation may be a compensatory response to impaired ER function.

The TOR signaling pathway was found to be significantly over-represented by the downregulated genes. TOR is a conserved serine–threonine kinase that senses growth factor or nutrient status and promotes cell proliferation and survival, protein synthesis and metabolism in response to environmental changes (Wullschleger et al., 2006). Among the downregulated genes that are involved in TOR signaling, DNA damage-inducible transcript 4, also known as *redd1* (ddit4) encodes an inhibitor of mammalian TOR (mTOR) in response to hypoxia and nutrient restriction (Sofer et al., 2005). The base methyltransferase of 25S rRNA 2 homolog (*bmt2*) is an S-adenosylmethionine sensor that can sense methionine starvation and thus inhibit mTOR complex 1 (mTORC1) activation (Gu et al., 2017). Sestrin 1 (*sesn1*) is a P53 target gene that

inhibits mTOR upon genotoxic challenge (Budanov and Karin, 2008). Sesns are reported to protect organisms against DNA damage, oxidative stress, starvation, ER stress and hypoxia and play key roles in autophagy activation and apoptosis inhibition (Chen et al., 2022). Downregulation of the TOR signaling inhibitors may be acclimation responses of the cells to the stressful conditions caused by high dietary HI meal.

Feeding on high HI meal diets caused changes in the profiles of more than 1000 metabolites. The metabolomic data provide further insight into the mechanisms underlying the adverse effects of high dietary HI meal. The metabolite 4-thialysine (also known as L-thialysine) is accumulated in the liver of fish fed on high HI. L-thialysine is a cysteine derivative that is the S-(2-aminoethyl) analogue of *L*-cysteine. It has been reported to have cytotoxic effects (Jun et al., 2003) and can function as a protein synthesis inhibitor and a lysine 2,3-aminomutase inhibitor. Another high HI meal-induced metabolite, xanthurenic acid, a metabolite of the tryptophan oxidation pathway through kynurenine and 3-hydroxykynurenine, also has toxic and apoptotic properties (Gobaille et al., 2008). Accumulation of these toxic metabolites may be ascribed to the disturbances in liver function by the high HI meal diet.

Linoleic acid metabolism and alpha-linolenic acid metabolism were found to be enriched among the differential metabolites. The contents of linoleic acid, octadecatrienoic acid and stearidonic acid in the liver of the HI40 fish were significantly decreased compared to the controls. Linoleic acid is one the most abundant dietary polyunsaturated fatty acids (polyunsaturated fatty acids). It can be esterified to form polar lipids such as phospholipids that function as essential membrane components to maintain membrane fluidity (Whelan and Fritsche, 2013). After being released from phospholipids, linoleic acid can be enzymatically oxidized to generate a couple of derivatives involved in cell signaling (Whelan and Fritsche, 2013). Deficiency of linoleic acid can lead to growth retardation and fatty liver in humans (Connor, 1999). The decreased linoleic acid content in the liver of the HI40 fish may be related to higher liver lipid accumulation and reduced growth rate.

Furthermore, a couple of genes and metabolites involved in amino acid biosynthesis and metabolism were impacted by the high HI meal diet. For example, among the affected genes and metabolites involved in tryptophan metabolism, expression of the *tdo2a* gene and the content of 5-hydroxy-L-tryptophan were significantly decreased. Tdo2a has the ability to catalyze the tryptophan catabolic process to kynurenine. Kynurenine in turn can stimulate activation of the aryl hydrocarbon receptor (AhR)/AKT signaling pathway, thus resulting in increased cellular proliferation (Zhong et al., 2022). 5-hydroxy-*L*-tryptophan (5-HTP) is the immediate precursor in the biosynthesis of 5-hydroxy-tryptamine (5-HT, serotonin) from *L*-tryptophan (*L*-Trp) (Das et al., 2004). The decrease of 5-HTP and increase of *L*-Trp in the liver of the HI40 fish indicate that the efficiency of 5-HT generation may be reduced. Furthermore, 5-HT is a regulator of the immune system (Franco et al., 2021). This is consistent with the findings that the down-regulated genes are enriched in immune-related pathways.

5. Conclusion

Including too high a proportion of *H. illucens* meal reduced growth of *M. salmoides* in this study. Integrated metabolomic and transcriptomic analyses were employed to investigate the changes in metabolites and genes between the HI0 and HI40 groups. Distinct metabolic pathways were identified in the liver of large-mouth bass, mainly repressing immune function, cellular protein biosynthesis capacity and lipid metabolism, inducing ER stress. The depression of antioxidant capacity was also observed in fish fed diets with the replacement of dietary FM by HI. Furthermore, both tryptophan and L-cysteine related to cellular protein biosynthesis ability were significantly affected by HI level, suggesting that amino acid metabolism and its related two metabolites are potential biomarkers for *M. salmoides* fed diets with increased dietary HI. Overall, our study enhanced our understanding of the effects of dietary insect protein and provides new ideas for feed formulation optimization of *M. salmoides*.

Author contributions

Hao Sun designed this study, carried out the experiments and measurements, and drafted the manuscript. **Wenjing Dong** and **Guanglun He** conducted experiments, wrote the manuscript and analyzed the data. **Yong Long** revised manuscript and analyzed the data. **Yuanfa He** helped with the sample analysis. **Yongjun Chen:** Supervision, Formal analysis. **Shimei Lin** provided the ideas for the project, experiment design, paper revising. All the authors read and approved the final manuscript.

Declaration of competing interest

We declare that we have no financial and personal relationships with other people or organizations that can inappropriately influence our work, and there is no professional or other personal interest of any nature or kind in any product, service and/or company that could be construed as influencing the content of this paper.

Acknowledgments

This research was supported by the National Key R&D Program of China (2019YFD0900200), Chongqing Ecological Fishery Technology System, China (2023) and Chongqing fishery technology innovation union (CQFTIU2022-05). We thank Han Huang, Yexin Wei, and Tingting Zhang for their help during the experiment.

Appendix supplementary data

Supplementary data to this article can be found online at https://doi.org/10.1016/j.aninu.2024.03.014.

References

AOAC. Official methods of analysis. 18th ed. Gaithersburg, MD: AOAC International; 2005.

Anedda R, Melis R, Palomba A, Vitangeli I, Biosa G, Braca A, et al. Balanced replacement of fish meal with *Hermetia illucens* meal allows efficient hepatic nutrient metabolism and increases fillet lipid quality in gilthead sea bream (*Sparus aurata*). Aquaculture 2023;576:739862. https://doi.org/10.1016/j.aquaculture.2023.739862.

Antonopoulou E, Nikouli E, Piccolo G, Gasco L, Gai F, Chatzifotis S, et al. Reshaping gut bacterial communities after dietary Tenebrio molitor larvae meal supplementation in three fish species. Aquaculture 2019;503:628–35. https://doi.org/10.1016/j.aquaculture.2018.12.013.

Bindea G, Mlecnik B, Hackl H, Charoentong P, Tosolini M, Kirilovsky A, Fridman WH, Pages F, Trajanoski Z, Galon J. Cluego: a cytoscape plug-in to decipher functionally grouped gene ontology and pathway annotation networks. Bioinformatics 2009;25(8):1091–3. https://doi.org/10.1093/bioinformatics/btp101.

Bosi A, Banfi D, Moroni F, Ceccotti C, Giron MC, Antonini M, Giaroni C, Terova G. Effect of partial substitution of fishmeal with insect meal (*hermetia illucens*) on gut neuromuscular function in gilthead sea bream (*sparus aurata*). Sci Rep 2021;11(1):21788. https://doi.org/10.1038/s41598-021-01242-1.

Budanov AV, Karin M. P53 target genes sestrin1 and sestrin2 connect genotoxic stress and mtor signaling. Cell 2008;134(3):451–60. https://doi.org/10.1016/j.cell.2008.06.028.

Cardinaletti G, Randazzo B, Messina M, Zarantoniello M, Giorgini E, Zimbelli A, et al. Effects of graded dietary inclusion level of full-fat *Hermetia illucens* prepupae meal in practical diets for rainbow trout (*Oncorhynchus mykiss*). Animals 2019;9:251. https://doi.org/10.3390/ani9050251.

Chen S, Zhou Y, Chen Y, Gu J. Fastp: an ultra-fast all-in-one fastq preprocessor. Bioinformatics 2018;34(17):i884–90. https://doi.org/10.1093/bioinformatics/bty560.

Chen Y, Huang T, Yu Z, Yu Q, Wang Y, Hu J, Shi J, Yang G. The functions and roles of sestrins in regulating human diseases. Cell Mol Biol Lett 2022;27(1):2. https://doi.org/10.1186/s11658-021-00302-8.
Chu XH, Li MM, Wang GY, Wang KM, Shang RS, Wang ZY, et al. Evaluation of the low inclusion of full-fatted Hermetia illucens larvae meal for layer chickens: growth performance, nutrient digestibility, and gut health. Front Vet Sci 2020;7:585843. https://doi.org/10.3389/fvets.2020.585843.
Connor WE. Alpha-linolenic acid in health and disease. Am J Clin Nutr 1999;69(5):827–8. https://doi.org/10.1093/ajcn/69.5.827.
Das YT, Bagchi M, Bagchi D, Preuss HG. Safety of 5-hydroxy-l-tryptophan. Toxicol Lett 2004;150(1):111–22. https://doi.org/10.1016/j.toxlet.2003.12.070.
Esmaeili N, Carter CG, Wilson R, Walker SP, Miller MR, Bridle A, Symonds JE. Proteomic investigation of liver and white muscle in efficient and inefficient chinook salmon (Oncorhynchus tshawytscha): fatty acid metabolism and protein turnover drive feed efficiency. Aquaculture 2021;542:736855. https://doi.org/10.1016/j.aquaculture.2021.736855.
Esmaeili N, Carter CG, Wilson R, Walker SP, Miller MR, Bridle AR, Symonds JE. Protein metabolism in the liver and white muscle is associated with feed efficiency in chinook salmon (oncorhynchus tshawytscha) reared in seawater: evidence from proteomic analysis. Comp Biochem Physiol Genomics Proteomics 2022;42:100994. https://doi.org/10.1016/j.cbd.2022.100994.
Esmaeili N, Carter CG, Wilson R, Walker SP, Miller MR, Bridle AR, Young T, Alfaro AC, Laroche O, Symonds JE. An integrated proteomics and metabolomics investigation of feed efficiency in seawater reared chinook salmon (Oncorhynchus tshawytscha). Aquaculture 2023;562:738845. https://doi.org/10.1016/j.aquaculture.2022.738845.
Esmail S, Manolson MF. Advances in understanding n-glycosylation structure, function, and regulation in health and disease. Eur J Cell Biol 2021;100(7–8):151186. https://doi.org/10.1016/j.ejcb.2021.151186.
Fang H, Harris SC, Su Z, Chen M, Qian F, Shi L, Perkins R, Tong W. Arraytrack: an fda and public genomic tool. Methods Mol Biol 2017;1613:333–53. https://doi.org/10.1007/978-1-4939-7027-8_13.
Fischer H, Romano N, Renukdas N, Kumar V, Sinha AK. Comparing black soldier fly (*Hermetia illucens*) larvae versus prepupae in the diets of largemouth bass, Micropterus salmoides: Effects on their growth, biochemical composition, histopathology, and gene expression. Aquaculture 2022;546:737323. https://doi.org/10.1016/j.aquaculture.2021.737323.
Franco R, Rivas-Santisteban R, Lillo J, Camps J, Navarro G, Reyes-Resina I. 5-hydroxytryptamine, glutamate, and atp: much more than neurotransmitters. Front Cell Dev Biol 2021;9:667815. https://doi.org/10.3389/fcell.2021.667815.
Fronte B, Licitra R, Bibbiani C, Casini L, De Zoysa M, Miragliotta V, et al. Fishmeal replacement with *Hermetia illucens* meal in aquafeeds: effects on zebrafish growth performances, intestinal morphometry, and enzymology. Fishes 2021;6(3):28. https://doi.org/10.3390/fishes6030028.
Gobaille S, Kemmel V, Brumaru D, Dugave C, Aunis D, Maitre M. Xanthurenic acid distribution, transport, accumulation and release in the rat brain. J Neurochem 2008;105(3):982–93. https://doi.org/10.1111/j.1471-4159.2008.05219.x.
Gu X, Orozco JM, Saxton RA, Condon KJ, Liu GY, Krawczyk PA, Scaria SM, Harper JW, Gygi SP, Sabatini DM. Samtor is an s-adenosylmethionine sensor for the mtorc1 pathway. Science 2017;358(6364):813–8. https://doi.org/10.1126/science.aao3265.
He GL, Zhang TT, Zhou XM, Liu XP, Sun H, Chen YJ, et al. Effects of cottonseed protein concentrate on growth performance, hepatic function and intestinal health in juvenile largemouth bass, *Micropterus salmoides*. Aquacult Rep 2022;23:101052. https://doi.org/10.1016/j.aqrep.2022.101052.
Hirata T, Kizuka Y. N-glycosylation, the role of glycosylation in health and disease. 2021.
Jiang B, Tsao R, Li Y, Miao M, Food Safety. Food Analysis Technologies/Techniques. In: Van Alfen NK, editor. Encyclopedia of Agriculture and Food Systems. Oxford: Academic Press; 2014. p. 273–88. https://doi.org/10.1016/B978-0-444-52512-3.00052-8.
Jun DY, Rue SW, Han KH, Taub D, Lee YS, Bae YS, Kim YH. Mechanism underlying cytotoxicity of thialysine, lysine analog, toward human acute leukemia jurkat t cells. Biochem Pharmacol 2003;66(12):2291–300. https://doi.org/10.1016/j.bcp.2003.08.030.
Kim D, Paggi JM, Park C, Bennett C, Salzberg SL. Graph-based genome alignment and genotyping with hisat2 and hisat-genotype. Nat Biotechnol 2019;37(8):907–15. https://doi.org/10.1038/s41587-019-0201-4.
Li X, Qin C, Fang Z, Sun X, Shi H, Wang Q, Zhao H. Replacing dietary fish meal with defatted black soldier fly (*hermetia illucens*) larvae meal affected growth, digestive physiology and muscle quality of tongue sole (*cynoglossus semilaevis*). Front Physiol 2022;13:855957. https://doi.org/10.3389/fphys.2022.855957.
Liao Y, Smyth GK, Shi W. Featurecounts: an efficient general purpose program for assigning sequence reads to genomic features. Bioinformatics 2014;30(7):923–30. https://doi.org/10.1093/bioinformatics/btt656.
Livak KJ, Schmittgen TD. Analysis of relative gene expression data using real-time quantitative pcr and the 2(-delta delta c(t)) method. Methods 2001;25(4):402–8. https://doi.org/10.1006/meth.2001.1262.
Love MI, Huber W, Anders S. Moderated estimation of fold change and dispersion for rna-seq data with deseq2. Genome Biol 2014;15(12):550. https://doi.org/10.1186/s13059-014-0550-8.
Manirakiza P, Covaci A, Schepens P. Comparative study on total lipid determination using soxhlet, roese-gottlieb, bligh & dyer, and modified bligh & dyer extraction methods. J Food Compos Anal 2001;14(1):93–100. https://doi.org/10.1006/jfca.2000.0972.
Marco MD, Martínez S, Hernandez F, Madrid J, Gai F, Rotolo L, et al. Nutritional value of two insect larval meals (*tenebrio molitor* and *hermetia illucens*) for broiler chickens: Apparent nutrient digestibility, apparent ileal amino acid digestibility and apparent metabolizable energy. Anim Feed Sci Technol 2015;209:211–8. https://doi.org/10.1016/j.anifeedsci.2015.08.006.
Mohan K, Rajan DK, Muralisankar T, Ganesan AR, Sathishkumar P, Revathi N. Use of black soldier fly (*hermetia illucens* L.) larvae meal in aquafeeds for a sustainable aquaculture industry: A review of past and future needs. Aquaculture 2022;553:738095. https://doi.org/10.1016/j.aquaculture.2022.738095.
Morro B, Broughton R, Balseiro P, Handeland SO, Mackenzie S, Doherty MK, Whitfield PD, Shimizu M, Gorissen M, Sveier H, Albalat A. Endoplasmic reticulum stress as a key mechanism in stunted growth of seawater rainbow trout (*oncorhynchus mykiss*). BMC Genomics 2021;22(1):824. https://doi.org/10.1186/s12864-021-08153-5.
NRC (National Research Council). Nutrient requirements of fish and shrimp. Washington, DC: The National Academy Press; 2007.
Pang Z, Chong J, Zhou G, de Lima Morais DA, Chang L, Barrette M, Gauthier C, Jacques PE, Li S, Xia J. Metaboanalyst 5.0: narrowing the gap between raw spectra and functional insights. Nucleic Acids Res 2021;49(W1):W388–96. https://doi.org/10.1093/nar/gkab382.
Randazzo B, Zarantoniello M, Cardinaletti G, Cerri R, Giorgini E, Belloni A, Conto M, Tibaldi E, Olivotto I. *Hermetia illucens* and poultry by-product meals as alternatives to plant protein sources in gilthead seabream (*sparus aurata*) diet: a multidisciplinary study on fish gut status. Animals (Basel) 2021;11(3). https://doi.org/10.3390/ani11030677.
Rimoldi S, Gini E, Iannini F, Gasco L, Terova G. The effects of dietary insect meal from *hermetia illucens* prepupae on autochthonous gut microbiota of rainbow trout (*oncorhynchus mykiss*). Animals (Basel) 2019;9(4). https://doi.org/10.3390/ani9040143.
Sayers EW, Bolton EE, Brister JR, Canese K, Chan J, Comeau DC, Connor R, Funk K, Kelly C, Kim S, Madej T, Marchler-Bauer A, Lanczycki C, Lathrop S, Lu Z, Thibaud-Nissen F, Murphy T, Phan L, Skripchenko Y, Tse T, Wang J, Williams R, Trawick BW, Pruitt KD, Sherry ST. Database resources of the national center for biotechnology information. Nucleic Acids Res 2022;50(D1):D20–6. https://doi.org/10.1093/nar/gkab1112.
Shannon P, Markiel A, Ozier O, Baliga NS, Wang JT, Ramage D, Amin N, Schwikowski B, Ideker T. Cytoscape: a software environment for integrated models of biomolecular interaction networks. Genome Res 2003;13(11):2498–504. https://doi.org/10.1101/gr.1239303.
Sofer A, Lei K, Johannessen CM, Ellisen LW. Regulation of mtor and cell growth in response to energy stress by redd1. Mol Cell Biol 2005;25(14):5834–45. https://doi.org/10.1128/MCB.25.14.5834-5845.2005.
Thevenot EA, Roux A, Xu Y, Ezan E, Junot C. Analysis of the human adult urinary metabolome variations with age, body mass index, and gender by implementing a comprehensive workflow for univariate and opls statistical analyses. J Proteome Res 2015;14(8):3322–35. https://doi.org/10.1021/acs.jproteome.5b00354.
Wang BT, Wu HL, Dong YW, Jiang B, Li W, Su YL, Huang YH, Liu C. Effects of fishmeal substitution with hermetia illucens l on the growth, metabolism and disease resistance of micropterus salmoides. J Insects Food Feed 2022;8(11):1343–53. https://doi.org/10.3920/JIFF2021.0201.
Whelan J, Fritsche K. Linoleic acid. Adv Nutr 2013;4(3):311–2. https://doi.org/10.3945/an.113.003772.
Wullschleger S, Loewith R, Hall MN. Tor signaling in growth and metabolism. Cell 2006;124(3):471–84. https://doi.org/10.1016/j.cell.2006.01.016.
Xie S, Liu Y, Tian L, Niu J, Tan B. Low dietary fish meal induced endoplasmic reticulum stress and impaired phospholipids metabolism in juvenile pacific white shrimp, *litopenaeus vannamei*. Front Physiol 2020;11:1024. https://doi.org/10.3389/fphys.2020.01024.
Yu M, Li Z, Chen W, Rong T, Wang G, Wang F, et al. Evaluation of full-fat *hermetia illucens* larvae meal as a fishmeal replacement for weanling piglets: Effects on the growth performance, apparent nutrient digestibility, blood parameters and gut morphology. Anim Feed Sci Technol 2020;264:114431. https://doi.org/10.1016/j.anifeedsci.2020.114431.
Zhao L, Liang J, Chen F, Tang X, Liao L, Liu Q, Luo J, Du Z, Li Z, Luo W, Yang S, Rahimnejad S. High carbohydrate diet induced endoplasmic reticulum stress and oxidative stress, promoted inflammation and apoptosis, impaired intestinal barrier of juvenile largemouth bass (*micropterus salmoides*). Fish Shellfish Immunol 2021;119:308–17. https://doi.org/10.1016/j.fsi.2021.10.019.
Zhong C, Peng L, Tao B, Yin S, Lyu L, Ding H, Yang X, Peng T, He H, Zhou P. Tdo2 and tryptophan metabolites promote kynurenine/ahr signals to facilitate glioma progression and immunosuppression. Am J Cancer Res 2022;12(6):2558.